Biochimica et Biophysica Acta, 602 (1980) 355—375

BBA 78975

EFFECTS OF IONIC STRENGTH, SERUM PROTEIN AND SURFACE CHARGE ON MEMBRANE MOVEMENTS AND VESICLE PRODUCTION IN HEATED ERYTHROCYTES

W. TERENCE COAKLEY and J. OWEN T. DEELEY

Department of Microbiology, University College, Newport Road, Cardiff CF2 1TA (U.K.)

(Received February 19th, 1980)
(Revised manuscript received June 30th, 1980)

Key words: Membrane bending; Interfacial instability; Vesicle formation; Surface charge density; Bilayer couple; Spectrin phosphorylation; (Erythrocyte)

Summary

Morphological changes and fragmentation of human erythrocytes heated at various rates through the spectrin inactivation temperature have been examined by cinephotomicroscopy. Most cells heated in 0.20 ionic strength buffered saline developed a wavy disturbance along the cell rim when heated. Vesicles developed from the crests of the growing waves within 0.3 s of the initiation of a wave when the heating rate was 1°C/s. At an ionic strength of 0.02, only 48% of the cells developed a wave outline. The average number of waves per cell was half that at 0.2 ionic strength. When the cell surface charge was reduced by neuraminidase treatment, only 12% of the cells fragmented. Bovine serum albumin or homologous plasma also reduced fragmentation. The dependence of the wave growth on ionic strength and surface charge was broadly consistent with theoretical predictions for the growth of a displacement instability on a low interfacial tension interface. Attention has been paid to the importance of bending energy in the development of the wave. Where wave development was suppressed, the morphological changes due to heating appeared to involve membrane internalization in the region of the cell dimple.

Introduction

The changes in erythrocyte morphology and deformability which occur at temperatures in excess of 48°C are believed to be related to the thermal denaturation of spectrin, an erythrocyte membrane cytoplasmic-face extrinsic protein [1—3]. The peak of the first thermal transition of spectrin occurs

at 49.5°C [3]. The phosphorylation of spectrin in human erythrocyte membrane preparations incubated for 10 min is slightly decreased at 46°C and totally inhibited at 50°C [4]. Schultze [5] developed a heatable microscope stage to observe the morphological changes that occurred in heated erythrocytes. Among his detailed observations, made over 100 years ago, he recorded that at 52°C initially superficial indentations on the rim of some red blood cells deepened and rapidly led to the production of spherical fragments which usually remained in contact with the cell, as if on a fine stem. Subdivision of heated erythrocytes can occur without loss of haemoglobin. When cells are heated over a range of heating rates, in an environment which protects them against the effects of shear stress, the threshold temperature for haemolysis is over 10°C higher than the threshold temperature for morphological change [6].

Some recent cinephotomicroscopic observations of erythrocytes during heating led us to examine heated erythrocytes as a model system in which to study the interfacial stability of membranes [6—9].

The theoretical study of interfacial instability requires that the initial state of a system be specified and then that the response of the system to a perturbation of that initial stage be examined [10]. Perturbations can originate outside the system, as with various types of vibration, or inside, when random thermal motion leads to small fluctuations in interfacial composition or shape. The perturbations that occur are, therefore, at least partially dependent on chance. The deformation of a plane interface which arises from a small perturbation can be expressed as a Fourier integral so that it suffices, for purposes of stability analysis, to determine the response of the system to simple periodic sine and cosine disturbances. If all of the simple perturbations die out so will the general perturbation, and the initial state is stable. However, if a simple sine or cosine disturbance of any wavelength grows then the system is unstable [10]. In a system which is unstable over a range of wavelengths, the wavelength with the fastest growth rate will dominate the instability growth. Analysis of large perturbations may show whether the unstable situation approaches a new steady state with the interface deformed but intact, or whether 'catastrophic' instability occurs with the original interface breaking up to form drops or particles [10].

In our previous work, the growth of displacement instabilities on a cylindrical form on one fluid immersed in another, a classical system for studying droplet formation by interfacial forces [11], was mimicked by applying hydrodynamic stress to heated cells attached to a glass surface [7—9]. Some cells were pulled away from the surface by the flow stress. A ring of membrane-enclosed cell contents often remained attached to the glass and a tether from the ring restrained the main cell body in the suspending liquid phase. The tether, a membrane tube enclosing cell contents, changed into a string of connected vesicles as the cell moved. A ring of membrane-enclosed material which remained attached to the glass also broke up into regularly spaced vesicles. The spacing of the vesicles was less than that predicted by theory [11] for the breakup of an uncharged viscous cylinder of one liquid immersed in another. Measurements, obtained mainly from the rings attached to the glass, of the growth rate of the displacement instability which led to vesicle

formation suggested a value of about 1.0 μN/m for the effective interfacial tension [8].

In the present paper, we report some observations on the fragmentation of erythrocytes heated at different rates through the first thermal transition of spectrin, in the absence of any externally applied hydrodynamic stress. The cells were heated in an environment which protected them from the influence of temperature-gradient-induced currents which can confuse the interpretation of cell breakdown [6]. Attention is directed to the influence of suspending phase ionic strength, of surface charge, and of the albumin content of the bulk phase on the response of the cell to inactivation of its cytoskeletal elements. The results are examined in the light of current ideas on interfacial stability. Our primary interest is not in determining the properties of erythrocytes at physiological temperatures. Rather, the heated erythrocyte is studied as a model membrane system from which understanding of the factors which influence membrane bending, membrane displacement instability and therefore membrane stability, may emerge.

Materials and Methods

Human erythrocytes were collected by finger prick into phosphate-buffered saline. The buffer was made up of 145 mM NaCl in 5 mM KH_2PO_4 and the pH was adjusted with K_2HPO_4 to pH 7.4. The collected cell concentration was about 5.10^7 cells/ml. Cells suspended as above will be termed 'as collected' cells. When preparing samples in which to examine the influence of the suspending phase on the response of the cells to heat the collected cells were centrifuged in a bench centrifuge, the supernatant was decanted and the cells were resuspended in an equal volume of suspending fluid at a pH of 7.4. All cells were stored at room temperature and were heated within 2 h of being collected, unless otherwise stated.

The ionic strength of the resuspending medium was varied by prior mixing of appropriate volumes of buffer and a 5% (w/v) solution of sorbitol [12]. The ionic strength of the buffer was 0.20 when allowance was made for the contribution of the phosphate salts.

The surface charge of the erythrocytes was reduced by resuspending the centrifuged cells in phosphate-buffered saline containing 0.05 to 0.5 units of activity of neuraminidase (EC 3.2.1.18, Type VI, Sigma Ltd.) per ml and incubating at 37° C for periods of up to 30 min. Following incubation the cells were centrifuged immediately in a bench centrifuge. The supernatant was decanted and the cells were resuspended in buffer and stored on ice. The electrophoretic mobility of the cells was measured in a modified Rank apparatus [13]. Measurements were made on at least ten cells from each sample. The electrophoretic mobility of neuraminidase-treated cells was expressed as a percentage of the mobility of control cells which had been incubated in buffer at 37° C. The electrophoretic mobilities were measured within 2 h of incubation.

The influence of bovine serum albumin on the morphological changes resulting from heating was examined following resuspension of centrifuged cells in buffer containing different concentrations of albumin (Fraction V, Armour Ltd., Eastbourne, U.K.).

Samples from cell suspensions prepared for morphological-change studies were drawn by surface tension into rectangular glass microcapillaries of 0.1 mm wall thickness, 0.1 mm pathlength and 1.2 mm width (Microslides, Camlab Ltd.). A heating device which consisted of two thin platinum T-piece electrodes attached to a microscope slide was positioned on a microscope stage. The microcapillary containing cell suspension was placed between the platinum electrodes. A cover slip was placed on the microcapillary and conducting saline was introduced between the cover slip and the microscope slide. The cells settled on the microcapillary surface during a 3 min waiting period. 'Glass-effect' echinocyte formation was rarely observed in the microcapillaries. The conducting saline was heated at a preset rate from room temperature by current from a 20 kHz power supply which was connected to the platinum electrodes. A bead thermistor close to the microcapillary monitored temperature during heating. The thermistor was in one arm of a Wheatstone bridge. The bridge output was measured on a potentiometric chart recorder. Heating rates were controlled by drawing a heating profile on the chart recorder paper and adjusting the input from the heating power supply so that the bridge output matched the preset profile. Further details and a sketch of the heating system are available elsewhere [8].

The effects of heating were recorded in preliminary studies by still photography of microscope fields before and after the temperature had passed through the spectrin melting temperature. Cine records were obtained at 16 frames/s with continuous illumination. Sequences recorded at 50 frames/s were illuminated by 15-μs exposure stroboscopic flashes from a Strobex 99 system (Chadwick-Helmuth). Cine records of the morphological changes were examined with a cine motion analyser. The number of waves on the periphery of a cell was scored by counting the protuberances which developed on the cell boundary as the morphological changes began. Protuberances did not develop all along the circumference of some cells, but cells on which waves grew on more than half of the rim were scored as having the number of waves which would result if the spacing of protuberances were similar over the whole circumference. The estimation of the number of waves per cell was carried out 'blind' in that the assessor was unaware of the nature of the suspending medium when examining the sequences.

Results

A number of sequences illustrating the development of wave-like profiles on cells as they were heated through the spectrin inactivation temperature are shown in Fig. 1. The first frame in each of the four sequences was taken when the temperature was just below the temperature at which morphological changes first became apparent. The cell in Fig. 1a, taken from a sample which was suspended in 0.02 ionic strength buffer with sorbitol, gradually took up a square shape and a four-wave pattern developed on the cell perimeter. The time interval from the third to the thirteenth frames of sequence (a) was 0.7 s, representing a bulk temperature change of 0.7°C. The sequence in Fig. 1b illustrates a development, best described as a five-wavelength disturbance, on the rim of a cell from an as collected sample. The total period

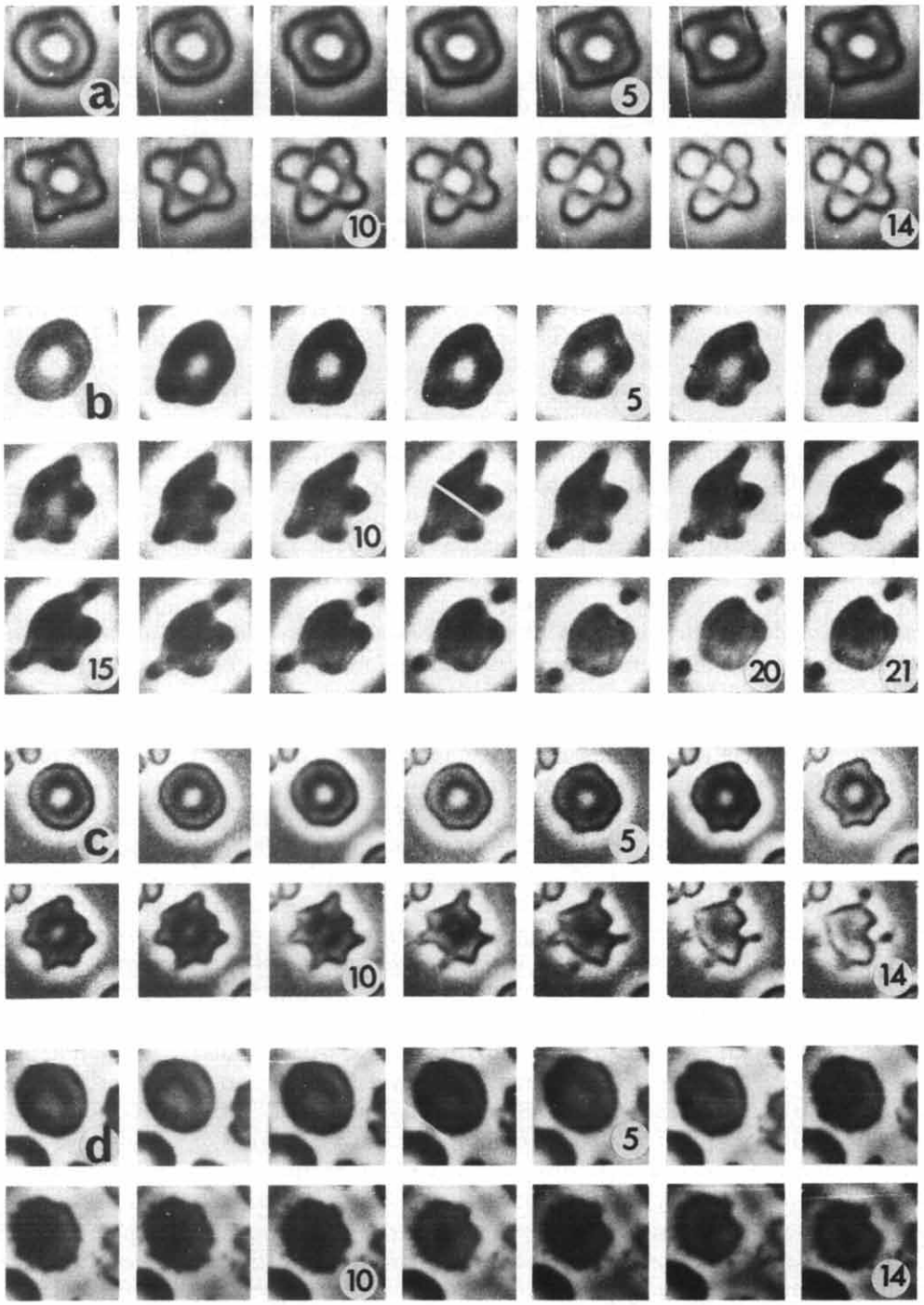

Fig. 1. (a, 1—14) Successive frames (16 frames/s) of a cell in 0.02 ionic strength buffer at a heating rate of 1°C/s. (b, 1—21) Successive frames (16 frames/s) of an as collected cell at a heating rate of 0.33°C/s. The line drawn on frame 11 shows the axis of symmetry of the wave development. (c, 1—14) Alternate frames (50 frames/s) of an as collected cell at a heating rate of 1°C/s. (d, 1—14) Successive frames (16 frames/s) of a washed cell in 0.2 ionic strength buffer at a heating rate of 1°C/s.

from frame 2 to frame 20 was 1.15 s, corresponding to a bulk temperature change of 0.35°C at the experimental heating rate. The wave development has an axis of symmetry which is drawn on frame 11. Vesicles develop almost simultaneously on the two most prominent waves on the cell. Both vesicles form over a period of 0.25 s, a time interval similar to that for vesicle formation on other cells in the same film field. Some other cells which developed a five-wave profile had a more regular star-like appearance. The peaks of the waves on these cells also developed vesicles at the wave crests. Fig. 1c illustrates the development of a seven-wave profile on a cell from an as collected sample. The time interval from frame 4 to frame 11 was 0.28 s, representing a bulk temperature increase of 0.28°C. Vesicles were produced from the four most prominent wave crests. The cell in Fig. 1d was in 0.20 ionic strength buffer. A short wavelength disturbance developed over a large section of the cell rim. The four cells presented in Fig. 1 have the growth of a regular wave pattern as a common feature. The evidence for the influence of environmental factors in determining the number of waves per cell will be presented later.

Some cells which illustrate aspects of wave development and vesicle production are presented in Fig. 2. Fig. 2a—d illustrates the regular spacing of disturbances which grew even on a limited section of the cell perimeter. Fig. 2a, b and particularly d show wave growth occurring selectively on straighter parts of the outlines of cells which did not have a circular shape on initially settling on the glass surface. The direction of the initially straight part of the cell in Fig. 2d is drawn on the fourth frame of that sequence. The growing disturbance on this cell can be seen to have an outline which is approximately sinusoidal. Microscopic examination of samples after heating often revealed the presence of a single vesicle on the side of a cell. In sixteen cases in which the development of a single vesicle was examined by cine-motion analysis, the development of a wave pattern as in Fig. 2e and f was seen before the disturbance at one area of the cell profile grew to a sufficiently high amplitude that a vesicle was pinched off. We found the sequence of Fig. 2g of interest because at a particular stage of heating (frames 1—3) one vesicle had been produced and an indentation was beginning to grow inwards at another point on the periphery. In the following four frames, a second vesicle was produced from a corner of the growing indentation. The arrow in frame 5 of Fig. 2g shows the wave growth which contributed to the formation of the second vesicle. It appears as though the first vesicle and the corner of the indentation had acted as boundaries for the growth of the wave between those two points. Inspection of Figs. 1 and 2 shows that in all cases in which vesicles were produced, the development was preceded by the growth of a wave from a base which was longer than the eventual diameter of the vesicle. In no case has a vesicle been detected developing by a ballooning mechanism to a diameter larger than the scale of the initial disturbance on the cell rim. In one case, a single vesicle developed from a single wave (broad-base) swelling on the side of what otherwise appeared to be a circular profile. However, superimposing projections of the cell image during development of the swelling showed a very low amplitude five-wave development on the cell periphery, but only one of the crests grew to produce a vesicle. This observation suggests that the structural weakness which led to the wave growth at only one region was of dimensions much

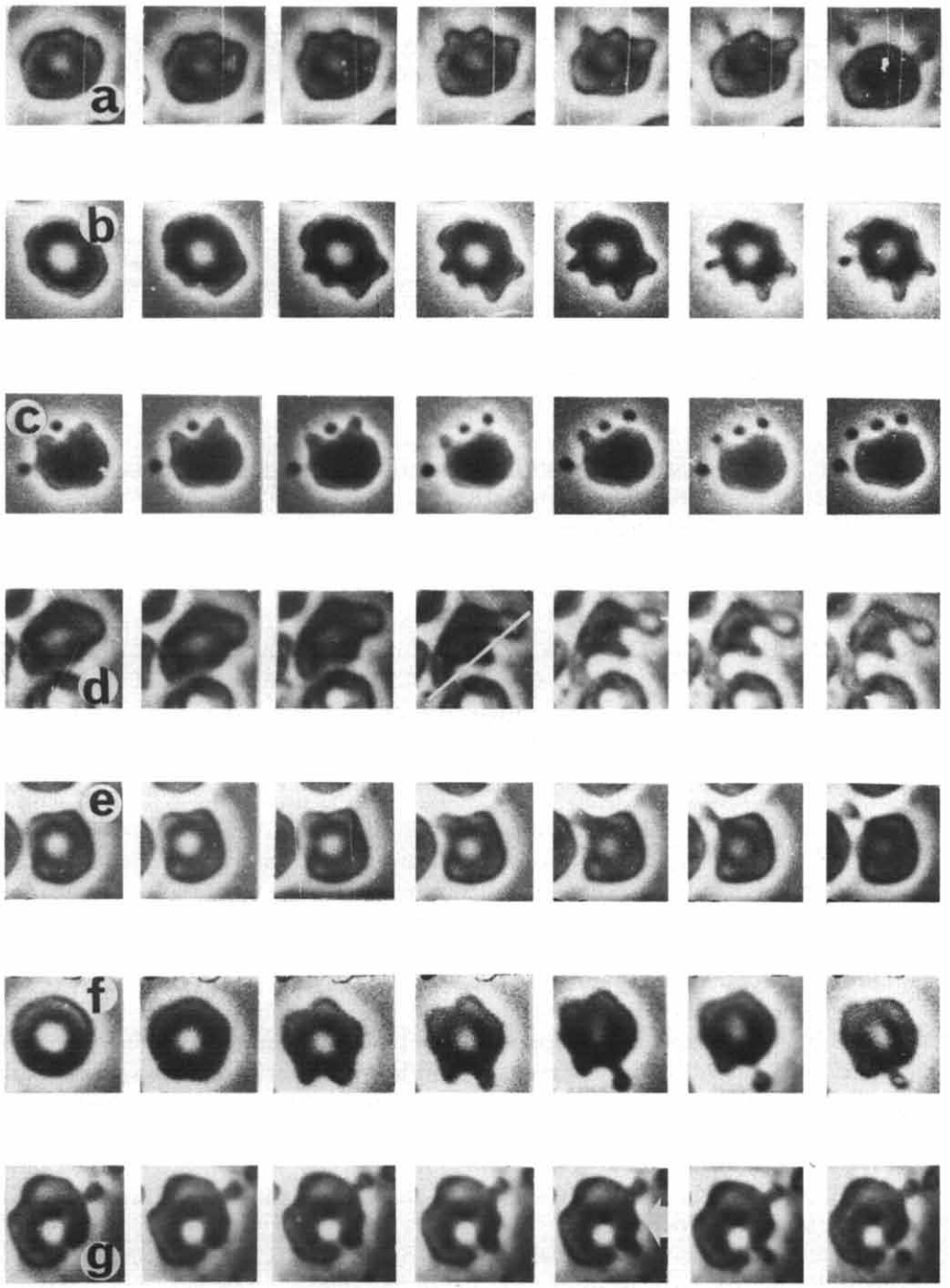

Fig. 2. Successive frames (4 frames/s) of an as collected cell at a heating rate of 0.08°C/s. (b) Alternate frames (50 frames/s) of a cell in 0.2 ionic strength buffer at a heating rate of 1°C/s. (c) Alternate frames (50 frames/s) of a cell in 0.2 ionic strength buffer at a heating rate of 1°C/s. (d) Successive frames (4 frames/s) of an as collected cell. The unstable disturbance can be seen growing about the line drawn on frame 4. (e) Successive frames (4 frames/s) of an as collected cell at a heating rate of 0.08°C/s showing the development of a single vesicle. (f) Selected frames of an as collected cell to show the initial wave development and the final single vesicles form. (g) Selected frames of an as collected cell to show the wave development of a second vesicle. The arrow in frame 5 shows the wave growth which preceded the formation of the second vesicle.

TABLE I

THE DISTRIBUTION OF 'NUMBER OF WAVES PER CELL' IN FOUR SAMPLES OF DIFFERENT IONIC STRENGTHS, HEATED AT 1°C/s

The 'zero waves per cell' class represents the percentage of cells which did not develop a wavy outline. The mode and 95% confidence limits for the mean number of waves per cell were determined from those cells which developed a wavy outline.

Ionic strength	Number of cells scored	Zero waves per cell (%)	Number of waves per cell		
			Range	Mode	95% confidence limits of the mean
0.2	46	0	7—14	11	10.1—11.3
0.12	46	22	4—13	9	7.9— 9.5
0.06	35	43	3— 9	4	4.7— 6.4
0.02	107	52	4— 9	4	4.7— 5.4

greater than the molecular scale and that all of the rim had participated in the initial very low amplitude five-wave disturbance.

The variation of the wave response of cells suspended in different ionic strength buffers was obtained from cine records and is summarized in Table I. It can be seen that the fraction of cells which did not develop a wave during heating (waves/cell = 0) increased from 0 to 0.52 as the ionic strength was decreased from 0.20 to 0.02. The behaviour of cells which did not develop a wave outline is discussed in more detail later. An average number of waves per cell was calculated for those cells which developed a wave and the 95% confidence limits of the mean are shown for each ionic strength in Table I. The mean number of waves per cell decreased from 10.7 to 5.1 when the ionic strength was changed from 0.20 to 0.02. The results presented in Table I were based on film records obtained from samples prepared from a single batch of blood. The results for each ionic strength were obtained from two to five different heated samples. The mean number of waves per cell tended to increase with time as the blood aged. The order of treating samples at different ionic strengths was varied so that the time-dependent increase in waviness did not unduly distort the dependence of waviness on ionic strength shown in Table I. A typical sequence of morphological changes in a 0.20 ionic strength sample on heating through the spectrin inactivation temperature (Fig. 3a) is contrasted with a 0.02 ionic strength sample in Fig. 3b. The samples were prepared from the same batch of blood and the heating rates were identical. The association of the higher number of waver per cell with the higher ionic strength is clear from Fig. 3. Examples of the development of individual fragmentation patterns can be observed by following the fate of single cells through the sequences of Fig. 3.

The result of a cine-film analysis of the response of control and neuraminidase-treated cells to heat is shown in Table II. The heating and the electrophoretic mobility measurement experiments were carried out concurrently and were completely within 2¼ h of the blood being drawn. It can be seen that the fraction of cells without wave development (wave/cell = 0) increased markedly as the relative cell charge decreased. The average number of waves per cell was significantly less in neuraminidase-treated cells than in controls.

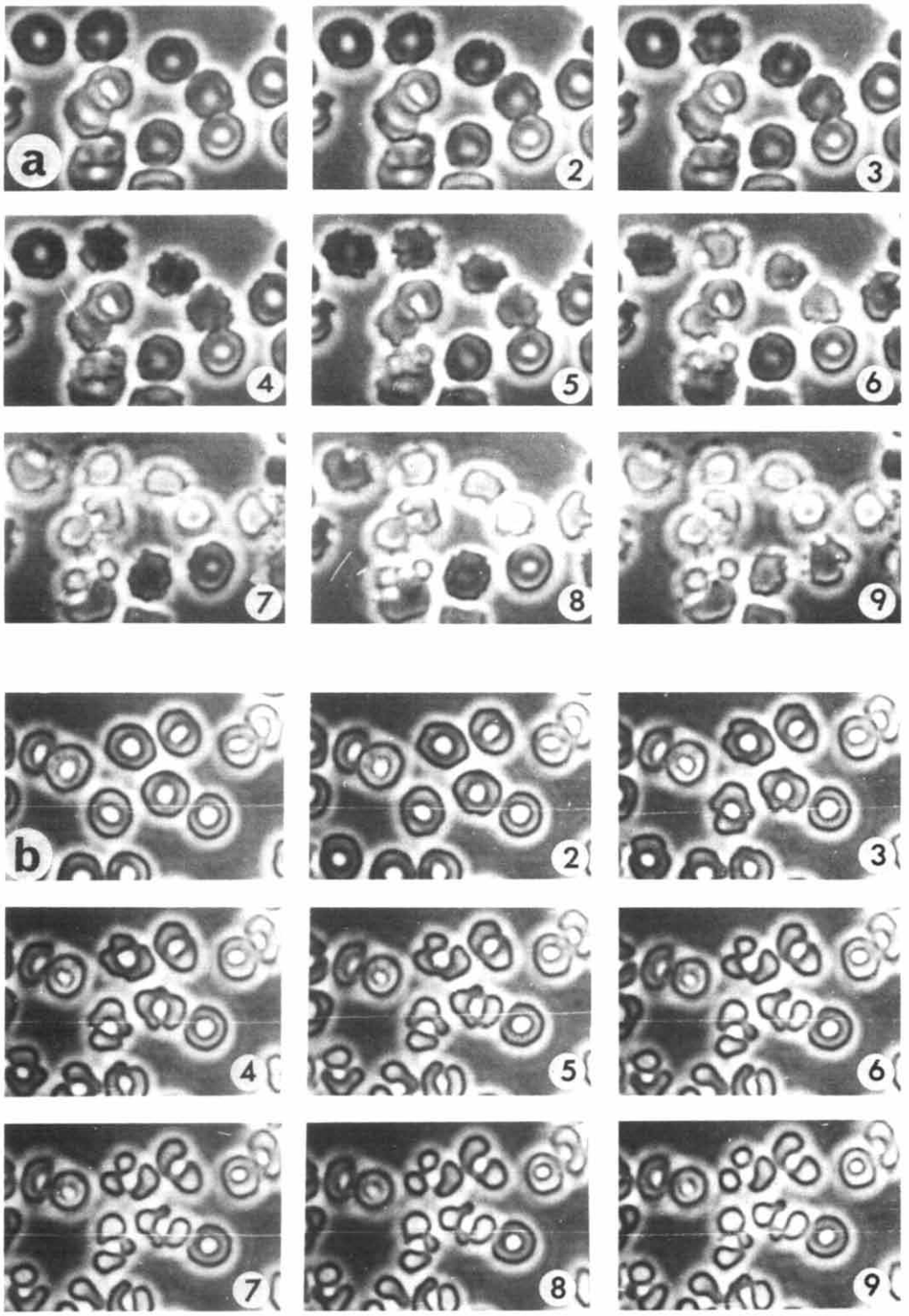

Fig. 3. (a, 1) Cells in 0.2 ionic strength buffer at the onset of fragmentation (16 frames/s) at a heating rate of 1°C/s: (a, 2—9) selected shots of the fragmentation pattern. The entire sequence (a, 1—9) took 1.32 s. (b, 1) Cells in 0.02 ionic strength buffer at the onset of fragmentation (16 frames/s) at a heating rate of 1°C/s: (b, 2—9) selected shots of the fragmentation pattern. The entire sequence (b, 1—9) took 1.32 s.

TABLE II

THE DISTRIBUTION OF 'NUMBER OF WAVES PER CELL' IN FOUR SAMPLES OF DIFFERENT SURFACE CHARGES, HEATED AT 1°C/s

The 'zero waves per cell' class represents the percentage of cells which did not develop a wavy outline.

Cell surface charge relative to control	Number of cells scored	Zero waves per cell (%)	Number of waves per cell		
			Range	Mode	95% confidence limits of the mean
1.00	64	6	6—15	11	9.9—11.0
0.51	24	38	5—12	8	7.6— 9.4
0.39	41	76	5—12	8	7.0— 9.4
0.34	24	88	6— 7	7	6.0— 7.4

TABEL III

THE INFLUENCE OF BOVINE SERUM ALBUMIN CONCENTRATION ON THE PERCENTAGE OF CELLS DEVELOPING A WAVY OUTLINE DURING HEATING IN 0.20 IONIC STRENGTH BUFFER

Albumin concentration (% w/v)	0	0.001	0.0033	0.0066	0.01
% of cells developing a wave	92	100	33	9	29
Total number of cells scored	24	24	24	22	38

TABLE IV

THE DISTRIBUTION OF 'NUMBER OF WAVES PER CELL' ON HEATING CELLS WHICH HAD BEEN WASHED AND RESUSPENDED IN 0.2 IONIC STRENGTH BUFFER COMPARED WITH THE DISTRIBUTION IN CELLS HEATED AS COLLECTED IN ABOUT 1% HOMOLOGOUS PLASMA

Cells	Number of cells scored	Zero waves per cell (%)	Number of waves per cell		
			Range	Mode	95% confidence limits of the mean
Washed and resuspended in buffer	231	7	3—17	10	9.0—9.7
As collected	158	27	4—11	6	6.0—6.6

TABLE V

THE INFLUENCE OF HEATING RATE ON THE AVERAGE NUMBER OF WAVES PER CELL AND ON THE AVERAGE TIME FOR A DISTURBANCE TO GROW FROM THE FIRST APPEARANCE OF A WAVE FORM TO THE FINAL FRAGMENTED SHAPE, FOR CELLS IN 0.2 IONIC STRENGTH BUFFER AND FOR AS COLLECTED CELLS

The 95% confidence limits for the averages are included.

Heating rate (°C/s)	Cells in 0.2 ionic strength buffer		As collected cells	
	Average number of waves/cell	Average time for disturbance development (s)	Average number of waves/cell	Average time for disturbance development (s)
1.0	9.1 ± 1.0	0.42 ± 0.04	5.6 ± 0.6	0.59 ± 0.14
0.1	7.9 ± 1.1	2.7 ± 0.8	5.7 ± 0.7	2.7 ± 0.4

The effect, on wave development on cells, of the presence of bovine serum albumin in the suspending medium is shown in Table III. Wave development was inhibited at concentrations of albumin of 0.003% (w/v) and greater. Again, the percentage of cells developing a wave pattern at any concentration of albumin increased as the sample aged. Results generally consistent with those of Table III were obtained when blood from other batches was heated after resuspension in a range of concentrations of albumin.

Table IV compares the response of cells in 0.20 ionic strength buffer with the response of as collected cells. The data was pooled from comparisons carried out on a number of different batches of cells. It can be seen from Table IV that a larger proportion of as collected cells do not develop waves and that the average number of waves per cell is less for the as collected cells than for the cells in buffer. A separate experiment showed that centrifugation and resuspension during the preparation of cells in buffer were not responsible for the different behaviour of those cells from as collected cells.

The influence of heating rate on the time required for a cell to fragment and on the average number of waves per cell was examined for cells heated in buffer and cells heated as collected. It can be seen from Table V that the average number of waves per cell was again greater for cells in buffer than for cells as collected, but that for each environmental condition the number of waves per cell was not strongly dependent on the heating rate.

The heating rate had a marked effect on the average time required for a wave pattern to grow to the final fragmentation form. The 95% confidence limits on the ratios of the fragmentation times at the two heating rates are $(6.4 \pm 2.1) : 1.0$ and $(4.6 \pm 1.3) : 1.0$ for cells heated in buffer and for cells as collected, respectively. The results imply a strong dependence of the fragmentation time on the rate of loss of cytoskeletal structure and function. However, since the ratios of fragmentation times are less than the 10 : 1 ratio of the reciprocals of the heating rates, the fragmentation time at the higher heating rate may be approaching a measure of the fragmentation time which would be obtained if the loss of the cytoskeletal function were instantaneous.

The following experiment was carried out to determine if attachment of cells to the glass surface of the microcapillary had a marked effect on either the number of waves per cell or the disturbance growth rate. An empty microcapillary was placed on the heating microscope slide and prepared for application of heat as if it contained cells. A drop of cells in buffer or a drop of as collected cell suspension was brought to the open end of the microcapillary. The cell suspension was drawn into the microcapillary and heating was begun almost immediately at 1°C/s. After about 32 s, the temperature was close to that required for cell fragmentation and many of the cells were still in suspension. Cine-film records of the morphological changes of these cells in suspension showed that the number of waves per cell and the disturbance growth rates were similar to those observed earlier when the cells were resting on the glass surface.

Some examples of the behaviour of cells which did not fragment by growth of a wave in the radial direction in the horizontal plane are shown in Fig. 4. As would be expected from Tables I—IV, the sequences are of heated blood

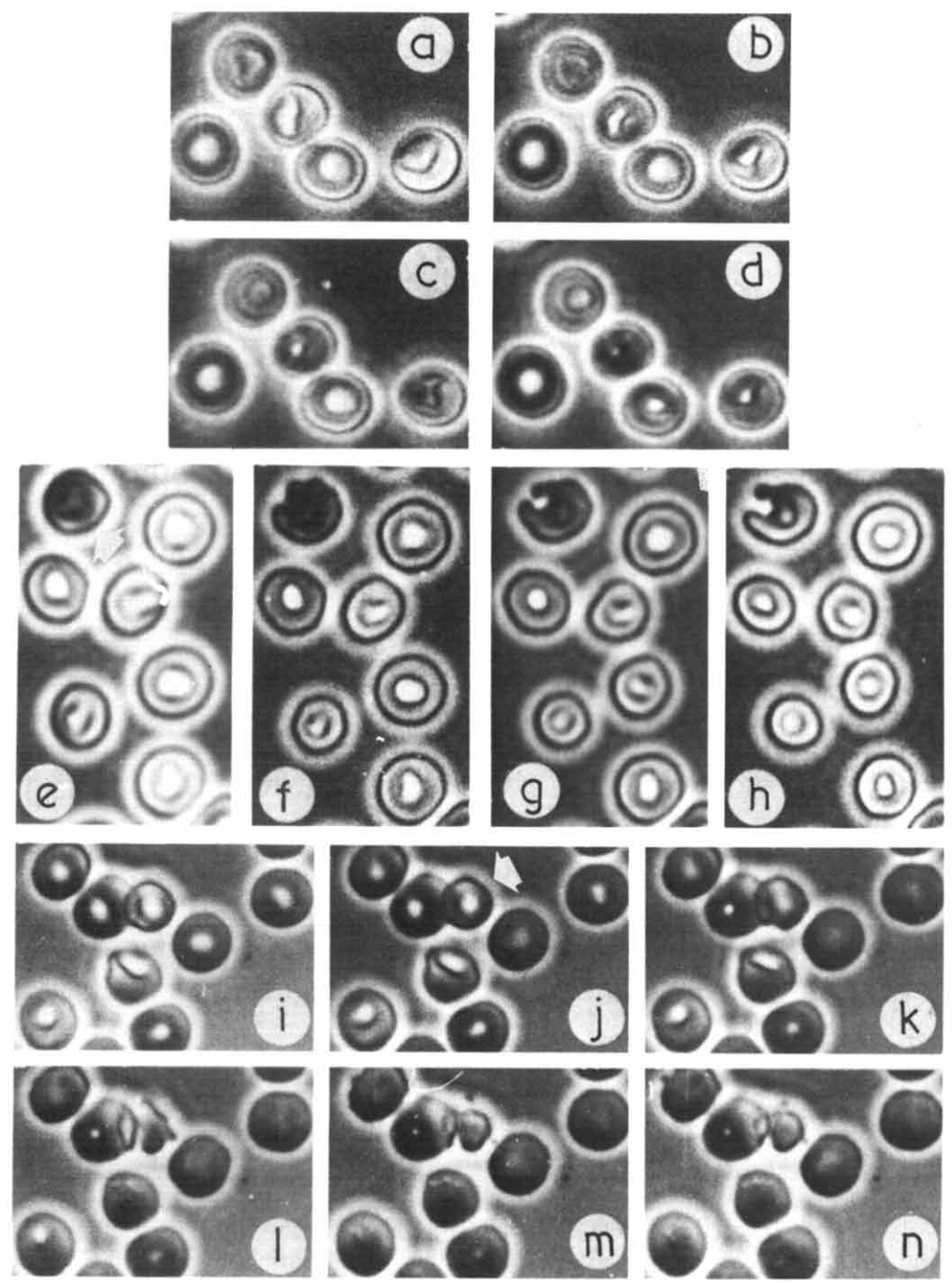

Fig. 4. Morphological changes in cells heated at 1°C/s under conditions which largely suppress the development of a wave on the cell rim. (a—d) Selected frames of cells suspended in 0.1% (w/v) bovine serum albumin; (a) $t = 0$, a control frame; (b) $t = 0.14$ s; (c) $t = 0.25$ s; (d) 0.76 s. (e—h) Selected frames of cells suspended in 0.02 ionic strength buffer; (e) $t = 0$, one frame before the arrowed cell had started to fragment; (f) $t = 0.35$ s; (g) $t = 0.68$ s; (h) $t = 1.23$ s. (i—n) Selected frames of cells that retained 34% of their charge following treatment with neuraminidase before washing and resuspending in buffer; (i) $t = 0$, a control frame before the arrowed cell in j had started to fragment at $t = 1.14$ s; (k) $t = 1.75$ s; (l) $t = 2.2$ s; (m) $t = 2.7$ s; (n) $t = 3.25$ s.

cells under conditions which reduce the incidence of waviness, i.e., high bovine serum albumin concentrations (Fig. 4a—d), low ionic strength of the suspending medium (Fig. 4e—h) and low surface charge density (Fig. 4i--n). The three sequences have in common the almost complete absence of waviness on the cell rims. If each sequence is examined by following individual cells from frame to frame it can be seen from Fig. 4 that the size of the cell dimple decreases markedly in some cells in going from frame a to frame d, a time interval of 0.76 s and a bulk temperature change of 0.76°C. In the low ionic strength sequence from Fig. 4e to h the diameters of the individual cells decreased as the cells were heated. The arrowed cell on frame e developed a wave and fragmented during the sequence showing that the rounding of the other cells in the frame occurred on passing through the cell fragmentation temperature. When the low surface charge density cells are followed individually from Fig. 4j to m, it can be seen that the cell dimples become much smaller during the sequence interval of 1.6 s and bulk temperature increase of 1.6°C. The fragmentation of the cell arrowed in frame 'k' again demonstrated that morphological changes occurred in the low charge density cells on passing through the cell fragmentation temperature. The three sequences suggest that in the absence of wave development the morphological change observed involves stomatocyte formation and in some cases membrane internalization. Fig. 4 and independent measurements show that the times for changes of individual cell diameters or dimples at a heating rate of 1°C/s are similar to the times required for the development of a wavy profile on cells passing through the spectrin inactivation temperature (Table V).

Discussion

We have shown that two major categories of morphological change can occur in human erythrocytes on heating through temperatures at which spectrin is partially denatured [3] and the phosphorylation of spectrin is reduced [4]. The essential difference between the two main responses is that in one case, a wave developing on the rim of the biconcave disc precedes fragmentation, while in the second case no wave develops on the rim, the morphological changes involve the cell dimple and the cell diameter may decrease.

The response of cells to heat under the environmental and surface charge conditions described above was quite repeatable. There was a restricted range of responses to heat under any one set of conditions in contrast to the greater variety of morphological changes reported in some previous studies [5,7,14]. Two changes in technique, the use of microcapillaries and of fixed heating rates, may have been responsible for the greater degree of reproducibility and the smaller number of types of morphological change observed here. We have previously noted [6] that the microcapillary environment protected cells against the effects of hydrodynamic stresses which are induced by temperature-gradient-driven flows in more open microscope slide environments. For instance, such flows can act on a vesicle so as to pull a chain of vesicles from a cell or can elongate a cell which is attached to glass so that the cell splits into two fragments separated by a small satellite bead [7]. In cells heated in the microcapillary system very few strings of vesicles were observed and

no cell fragmented by halving. Indeed, few wavy cells with less than four waves on their rims were detected (Tables I, II and IV). The practice of heating cells at predetermined rates gave more reproducible results than could be obtained by incubating cells on the microscope slide at a nominal fixed temperature. The improvement arose because there is a restricted range of temperature-time regimes over which heat will produce increased cell deformability. Two processes which affect membrane deformability operate during the exposure of erythrocytes to temperatures around 50°C. One process leads to greater deformability, presumably because of inactivation of spectrin, while the second process stiffens the membrane, possibly by cross-linking denatured protein [9]. The deformability of a cell incubated at a fixed temperature will depend on the net result of the two processes, so that the incubation temperature on the microscope slide would need to be very closely controlled. On the other hand, in our present system, heating rates can be selected which will guarantee that the cells will pass through a deformable state in each experiment.

Jones [15] lists values ranging from 5.7 to 0.08 mN/m for the measured tension at the surface of some cells and for the interfacial tension of lipid bilayers. The stability of interfaces with interfacial tensions 'less than a few mN/m' [16] has been extensively studied by Miller and Scriven [16,17,19,20] and Murphy [18]. Their work forms a useful background to an examination of the role of interfacial properties in the fragmentation of heated erythrocytes. An outline of their approach and results is now presented. When two bulk liquids are in contact and in equilibrium with each other, the forces on a molecule near the physical boundary are balanced but anisotropic. The pressure near the boundary is therefore anisotropic, in contrast to the isotropic pressure at points deep in the bulk liquids [18]. The presence of adsorbed molecules at an interface, or diffuse double layers near charged interfaces, can introduce further anisotropy at a boundary [16]. Murphy [18] extended earlier modifications by Buff [21] of Gibb's [22] surface-excess approach to the treatment of interfaces [23]. In the surface-excess scheme, the boundary between two bulk phases A and B is treated as a transition zone of finite thickness and significant internal structure. It is assumed that stress is transversely isotropic in the stratum-like regions, which can be spanned by a family of parallel surfaces. The bulk phases are extrapolated into the transition zone until they meet as if uninfluenced by each other at one of the parallel surfaces, arbitrarily chosen as the reference surface. Differences in properties between the actual and hypothetical extrapolated systems are assigned to the reference surface. The reference surface is designated 'the interface'. A boundary, C, is drawn on the reference surface and an orthogonal surface passing through C and extending into each bulk phase is constructed. This orthogonal surface plus two surfaces parallel to the reference surface are chosen on each side of, and very close to, the reference surface although at such a distance that they do not lie within the transition zone, to form a closed surface surrounding a volume, V, designated the interfacial region. This interfacial region contains the transition region plus small portions of each bulk phase (Fig. 5). The movement and deformation of the interfacial region can be followed by observing the motion of the reference surface.

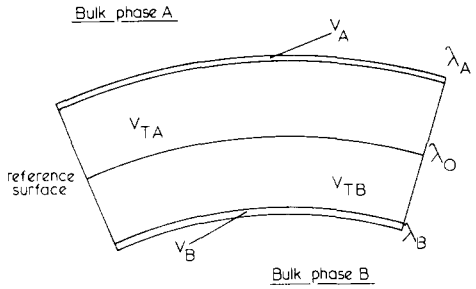

Fig. 5. A sectional view of an interfacial region of volume $V = V_A + V_{TA} + V_{TB} + V_B$. V_A and V_B are small parts of the bulk phases A and B, and V_{TA} and V_{TB} are those parts of the transition zone which are at the A and B sides of the reference surface at λ_0 where $\lambda = 0$. λ_A and λ_B are the perpendicular distances of the boundaries of the interfacial region from the reference surface.

Murphy [18] employed stratal integral theorems to relate integrals over the volume and outer surfaces of the stratal region in Fig. 5 to integrals over the reference surface. He derived expressions for (i) the interfacial tension, γ, where:

$$\gamma = \int_{\lambda_B}^{\lambda_A} (P_{A-B} - P_t)\, h d\lambda \tag{1}$$

(ii) a bending stress, H, where:

$$H = \int_{\lambda_B}^{\lambda_A} (P_{A-B} - P_t)\, \lambda d\lambda \tag{2}$$

and (iii) a torsion stress, K, where:

$$K = \int_{\lambda_B}^{\lambda_A} (P_{A-B} - P_t)\, \lambda^2 d\lambda \tag{3}$$

In the above expressions, λ represents distance in the normal direction from the reference surface, λ_A and λ_B are the distances from the reference surface to the boundaries of the interfacial region (in Fig. 5, λ_B has a negative numerical value). The pressure, P_{A-B}, takes the value of the pressure in the bulk phase A for surfaces on the A side of the reference surface, and at $\lambda = 0$. P_{A-B} takes the value of the pressure in bulk phase B at the B side of the reference surface. The term, P_t, is the tangential component of the pressure in the interfacial region at different values of λ. The area-scaling factor, h, in Eqn. 1 is a function of λ and the principal normal curvatures C_1 and C_2 of the reference surface [21].

The excess tangential stress can be written in pressure terms as $P_{A-B} - P_t$ [21] so that the interfacial tension is the integrated tangential stress over the interfacial region (Eqn. 1). The excess tangential stress in an interfacial region might be distributed as in Fig. 6. The bending term, H, is the integral of the first moment of the excess pressure about the reference surface (Eqn. 2). Since, by inspection of Fig. 6, this moment will not generally be zero (unless the

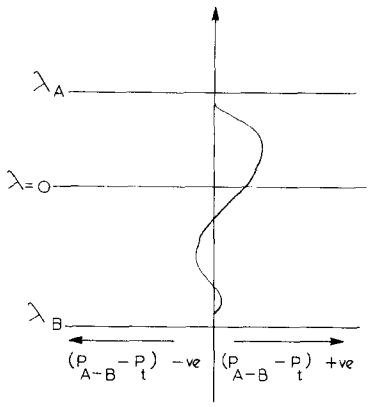

Fig. 6. A schematic representation of a possible distribution of the excess stress ($P_{A-B} - P_t$) within the interfacial region.

position of the reference surface is chosen to make it zero), Murphy [18] argued that this expression puts in quantitative form the concept of Bowcott and Schulman [24] that altering the conditions at one side of an interfacial region can affect net interfacial tension and interfacial bending. The torsion term (Eqn. 3) appears to play a role in breaking up the interface into droplets [18,25]. For low interfacial tension highly curved interfaces the free energy changes associated with bending or torsion of the interface can be comparable to the free energy changes associated, through area changes, with interfacial tension [18]. The concept of an interfacial region, which may be semi-permeable [22], as a discrete volume lying between two bulk regions is useful in the present context because the general treatment can include situations where surface-active material is adsorbed at the interface and where surface charge can introduce some structure by establishing a double layer [16]. The interfacial region concept also provides a framework within which chemical reactions and interfacial stability can be treated [16,18,20,22]. Since treatments of the stability of an interfacial region can be based on thermodynamics, it follows that the approach may be applied both to interfacial regions with liquid-like contents which can readily undergo area change, and to systems such as membranes where area change may be restricted by interfacial elasticity.

The condition that a closed system be in internal equilibrium is that the sum, E, of its internal energy, U, and potential energy, P, be a minimum, i.e.

$$\Delta E = \Delta(U + P) > 0 \tag{4}$$

for all virtual changes in the system from its equilibrium state. The biconcave disc may be considered as the stable equilibrium shape of the erythrocyte under physiological conditions. If a small wavy displacement of the surface leads to a decrease in the internal energy U or in the potential energy P of Eqn. 4 then a compensating change in U would be required to maintain the stable shape. Such a change could arise from the elastic response of the cytoskeletal elements. Evans and Hochmuth [26] have shown that at physiological temperatures, the response of the erythrocyte membrane to an externally applied stress is almost completely determined by the cytoskeleton, with the

bilayer making a negligible contribution. The cytoskeleton can be considered as an array of spectrin molecules cross-linked by actin monomers or very short filaments in which the cross-linking is regulated by the phosphorylation of spectrin [27]. A further stabilising increase in U might follow a disturbance if spectrin phosphorylation leads to increased cytoskeletal structure. The application of heat to a cell might, therefore, act to reduce the elasticity contribution to U following a disturbance, both as a direct result of a reduction in spectrin structuredness and by a thermal reduction in the phosphorylation of spectrin. The biconcave shape would then become unstable and the cell would take up a shape associated with a lower energy level over the whole surface.

The membrane area change which occurs when erythrocytes are stressed mechanically at physiological temperatures is small [28]. If some cytoskeletal resistance to stretching is retained in our heated cells, then this factor coupled with the shear and dilational elasticity of the bilayer could operate against the production of any significant surface area change during a morphological change. The morphological changes shown in Figs. 1—3 are all initiated by the growth of a wavy disturbance, often approximately sinusoidal, on the rim of the cell. Beads formed by a pinching of the wave-crest are an example of the development of an instability triggered by a displacement separate from the initial deformation which led to the growth of the wavy form. Following Murphy [18] and Evans [29] and taking the 'neutral surface', i.e., that surface in the interfacial region which does not undergo stretching if the region is subjected to pure bending, as a reference surface the growth of a wave around the rim of the red cell may be explained as follows. If a wavy disturbance can grow as an instablity, the interfacial region will bend and move in a direction normal to the cell rim. The bending interfacial region need not expand significantly but may pull membrane with it so that the area of the growing disturbance need not come from an expansion of the bilayer but could consist of membrane drawn along behind the wave-crest as the cell shape is altered.

The dependence of the morphological changes on ionic strength and surface charge (Tables I and II) suggest a role for electrical forces in determining the stability of the heated cells. The analysis of the influence of electrical forces on interfacial stability in physical and biological systems when charged interfaces or dipole layers are in contact with ionic solutions is becoming a subject of increasing interest [16,17,19,20,30—33]. The stability of a charged interface is influenced by diffuse-layer effects at low ionic strengths, while at ionic strengths in excess of 0.10 interactions occurring in the Stern layer within a distance from the surface of the order of the diameter of a hydrated ion become important [16,17,32].

In the low ionic strength analysis of the stability of a charged interface by Miller and Scriven [16,17], the diffuse layer was included in the interfacial region. The integral of Eqn. 1 over the full interfacial region was defined as the total interfacial tension, γ_T, while the integral over that part of the interfacial region which excluded the diffuse layer was called the phase interfacial tension, γ_P. The contribution of the diffuse layer to the total interfacial tension was denoted as $-\gamma_{DL}$.

The interface was first shown to become unstable to long wavelength distur-

bances when:

$$\gamma_T = \gamma_P - \gamma_{DL} \simeq 0 \tag{5}$$

For shorter wavelength disturbances, the interface was stable even if $\gamma_T < 0$. This stability could be interpreted, in the light of Murphy's [18] analysis of bending stress, as a resistance of the diffuse layer to bending [17,19]. For high ionic strengths (greater than 0.10) and high surface charge or dipole densities, the effects of interactions at the interface can destabilize a surface when the total interfacial tension is still positive [19,32].

The value of γ_{DL} taken from Verwey and Overbeek [34] has been given [17,18] as:

$$\gamma_{DL} = \delta_r \delta_0 \kappa (4kTn/\upsilon e)^2/2(1 - \eta^2) \tag{6}$$

where δ_r is the relative permittivity of the suspending medium, δ_0 is the permittivity of free space, κ is the reciprocal of the Debye length, k is Boltzmann's constant, T is the absolute temperature, υ is the valency of the ions of the suspending phase and e is the electronic charge. The term, η, is given [15] by:

$$\eta = \tanh(\upsilon e \Psi_0/4kT) \tag{7}$$

where Ψ_0 is the surface potential, which will be approximated by measured zeta potentials.

Reduction of the erythrocyte charge by neuraminidase treatment causes a marked increase in the number of cells which do not develop a wave on the rim (Table II). At constant ionic strength, a reduction in surface charge will reduce the zeta potential [15] thus reducing η (Eqn. 7). For the situation of interest here, $\eta < 1.0$ [12] so that a reduction in η will lead to a reduction in γ_{DL} (Eqn. 6) and will therefore reduce the destabilising influence of charge, in agreement with observation (Table II).

The effect on γ_{DL} of a 10-fold reduction in ionic strength can be determined from measurements obtained by Heard and Seaman [12] at ionic strengths of 0.145 and 0.0145. η has values of 0.341 and 0.136 and γ_{DL} has values of 0.193 and 0.085 mN/m for the lower and higher ionic strengths, respectively. For a constant surface charge situation, γ_{DL} increases as the ionic strength decreases so that γ_T will go to lower values (larger negative values) as the ionic strength decreases (Eqn. 5). However, the work necessary to bend the diffuse layer also increases as γ_{DL} increases [17,19] so that the diffuse layer can stabilize the interface even if γ_T is negative. The wavelength, λ_{fg}, of the fastest growing disturbance is given for the constant surface charge density condition [17,19] by:

$$\lambda_{fg} = 5\pi^2(3 - 4\eta^2 + \eta^4)(\gamma_{DL})/(-\gamma_T)(3\kappa^2)(1 + \eta^2) \tag{8}$$

A 10-fold reduction in ionic strength decreases the average number of waves per cell from 10.7 to 5.1 (Table I). The ratio of these averages (2.1 : 1.0) underestimates the effect of reducing the ionic strength because the average 5.1 relates only to those cells which developed a wave and it omits the influence of the cells, of which the membrane properties were such that a wave disturbance could not grow on the cell rim. If we assume that the instability

begins to grow at a fixed value of the quotient $(\gamma_{DL})/(-\gamma_T)$, then substituting the above values of η for ionic strengths of 0.145 and 0.0145 in Eqn. 8 gives the ratio for λ_{fg} over a 10-fold range of ionic strengths as 2.7 : 1. If the disturbance grows at a fixed value of $-\gamma_T$, then the ratio of the wavelengths at the two ionic strengths would be 4 : 1.

The increased wavelength at reduced ionic strengths is consistent with the view that diffuse double layers can influence the bending of interfaces. The reduction in external NaCl concentration will also effect the transmembrane potential as a consequence of changing the ratio of intracellular to extracellular Cl^- concentrations [35]. Available treatments for instability growth at charged interfaces do not include a term applicable to the assessment of the influence of transmembrane potential on membrane stiffness. Lew [36] proposed and Glaser [37] has recently demonstrated that transmembrane potential can influence the bending stiffness of erythrocyte membranes at physiological temperatures. We are presently investigating the relative contributions of surface potential and transmembrane potential to membrane stiffness, employing methods described by Hoffman and Laris [35] which allow the surface potential and transmembrane potential to be varied independently.

The number of cells developing a wavy outline decreased with increasing bovine serum albumin concentration (Table III). The wavelengths associated with as collected cells were longer than those associated with cells in buffer (Table IV). The interaction of albumin with the membrane is indicated by the ability of albumin to extract lysophosphatidylcholine and free fatty acids from the erythrocyte [38,39]. Such an interaction may induce a bending stress in the membrane leading to stomatocyte formation and to suppression of wave development on heating the erythrocytes.

The behaviour of cells which were heated through the spectrin inactivation temperature without wave development on the cell rim was shown in Fig. 4 for conditions of high albumin concentration, low ionic strength and low surface charge. Motion analysis of cine records of some cells under the above conditions suggests that internalization of the membrane is occurring at the cell dimple. There are some similarities between the erythrocyte crenation and internalization observed in our work and those changes induced at physiological temperatures by amphiphatic molecules. Both systems also have in common the suggestion that bending stresses play a role in producing the morphological changes. On the other hand, neuraminidase treatment of the erythrocytes does not appear to influence their response to drugs [40].

Conclusions

Our experimental measurements of the dependence of wave growth on ionic strength and cell surface charge are broadly consistent with the predictions of the theory of Miller and Scriven of the stability of a plane charged interface between inviscid bulk phases. Further experimental results are required to assess the role of transmembrane potential in membrane bending resistance.

The size of the erythrocyte, its relatively low internal viscosity and comparatively simple structure, together with the fact that its cytoskeletal function can be thermally impaired over a defined temperature range, combine to make

the heated cell one of the few model systems in which the growth of instabilities on membranes can be examined microscopically. The apparent connection between instability growth and membrane bending resistance suggests that the methods described here may have applications in the study of the role of some agents which modify membrane bending in those biological systems where bending occurs without the obvious wave growth seen in this work.

Acknowledgements

The authors are pleased to acknowledge useful discussion with D. Tilley. The Centre for Educational Technology and the Department of Zoology provided cinephotomicroscopy facilities. Dr. M.E.H. Holwill and Dr. A.J. Bater kindly provided access to stroboscopic cinemicroscopy equipment and an electrophoretic mobility measurement system, respectively. J.O.T.D. is grateful to the Medical Research Council for providing support during the course of this research.

References

1 Williamson, J.R., Shanahan, M.O. and Hochmuth, R.M. (1975) Blood 46, 611—624
2 Rakow, A.L. and Hochmuth, R.M. (1975) Biophys. J. 15, 1095—1100
3 Brandts, J.F., Erickson, L., Lysko, K., Schwartz, A.T. and Taverna, R.D. (1977) Biochemistry 16, 3450—3454
4 Mohandas, N., Greenquist, A.C. and Shohet, S.B. (1978) in Progress in Clinical and Biological Research (Brewer, G.J., ed.), Vol. 21, pp. 453—477, Alan R. Liss, New York
5 Schultze, M. (1865) Arch. Mikrosk, Anat. 1, 1—42
6 Coakley, W.T., Bater, A.J., Crum, L.A. and Deeley, J.O.T. (1979) J. Therm. Biol. 4, 85—93
7 Coakley, W.T., Bater, A.J. and Deeley, J.O.T. (1978) Biochim. Biophys. Acta 512, 318—330
8 Crum, L.A., Coakley, W.T. and Deeley, J.O.T. (1979) Biochim. Biophys. Acta 554, 76—89
9 Deeley, J.O.T., Crum, L.A. and Coakley, W.T. (1979) Biochim. Biophys. Acta 554, 90—101
10 Miller, C.A. (1978) in Surface and Colloid Science (Matijevic, E., ed.), Vol. 10, pp. 227—293, Plenum Press, New York
11 Meister, B.J. and Scheele, G.F. (1967) AIChEJ. 13, 682—688
12 Heard, D.H. and Seaman, G.V.F. (1960) J. Gen. Physiol. 43, 635—654
13 Sutherland, W.H. and Pritchard, J.A.V. (1979) in Cell Electrophoresis, Clinical Applications and Methodology (Preece, A.W. and Sadolovic, D., eds.), pp. 421—430, Elsevier, Amsterdam
14 Ponder, E. (1950) J. Exp. Biol. 27, 198—209
15 Jones, M.N. (1975) Biological Interfaces, Elsevier, Amsterdam
16 Miller, C.A. and Scriven, L.E. (1970) J. Colloid Interface Sci. 33, 360—370
17 Miller, C.A. and Scriven, L.E. (1970) J. Colloid Interface Sci. 33, 371—383
18 Murphy, C.L. (1966) Thermodynamics of Low Tension and Highly Curved Interfaces, Ph.D. Thesis, University of Minnesota, Minneapolis, University Microfilms, Xerox, Ann Arbor
19 Miller, C.A. (1968) Interfacial Instability due to Electrical Forces in Double Layers, Ph.D. Thesis, University of Minnesota, Minneapolis, University Microfilms, Xerox, Ann Arbor
20 Miller, C.A. and Scriven, L.E. (1974) J. Colloid Interface Sci. 46, 477—490
21 Buff, F.P. (1956) J. Chem. Phys. 25, 146—153
22 Gibbs, J.W. (1928) The Collected Works of J. Willard Gibbs, Vol. 1, 2nd edn., pp. 55—349, Longmans Green, New York
23 Adamson, A.W. (1967) Physical Chemistry of Surfaces, Interscience, New York
24 Bowcott, J.E. and Schulman, J.H. (1955) Z. Elektrochem. 59, 283—290
25 Rosoff, M. (1978) Progr. Surf. Membrane Sci. 12, 405—477
26 Evans, E.A. and Hochmuth, R.M. (1977) J. Membrane Biol. 30, 351—362
27 Pinder, J.C., Ungewickell, E., Bray, D. and Gratzer, W.B. (1978) J. Supramol. Struct. 8, 439—466
28 Evans, E.A., Waugh, R. and Melnik, L. (1976) Biophys. J. 16, 585—595
29 Evans, E.A. (1974) Biophys. J. 14, 923—931
30 Spertell, R.B. (1976) J. Theor. Biol. 60, 197—208
31 Van Lamsweerde-Gallez, D., Bisch, P.M. and Sanfeld, A. (1978) Bioelectrochem. Bioeng. 5, 401—410

32 Bisch, P.M., van Lamsweerse-Gallez, D. and Sanfeld, A. (1979) J. Colloid Interface Sci. 71, 501—512
33 Van Lamsweerde-Gallez, D., Bisch, P.M. and Sanfeld, A. (1979) J. Colloid Interface Sci. 71, 513—521
34 Verwey, E.J.W. and Overbeek, J.T.G. (1948) Theory of the Stability of Lyophobic Colloids, Elsevier, New York
35 Hoffman, J.F. and Laris, P.C. (1974) J. Physiol. 239, 519—552
36 Lew, H.S. (1972) J. Biomech. 5, 399—408
37 Glaser, R. (1970) J. Membrane Biol. 51, 217—228
38 Shohet, S.B. (1977) in Hematology (Williams, W.J., Beutler, E., Erslev, A.J. and Rundles, R.W., eds.), pp. 190—196, McGraw-Hill, New York
39 Jay, A.W.L. (1975) Biophys. J. 15, 205—222
40 Sheetz, M.P. and Singer, S.J. (1974) Proc. Natl. Acad. Sci. U.S.A. 71, 4457—4461